Expanded View Figures

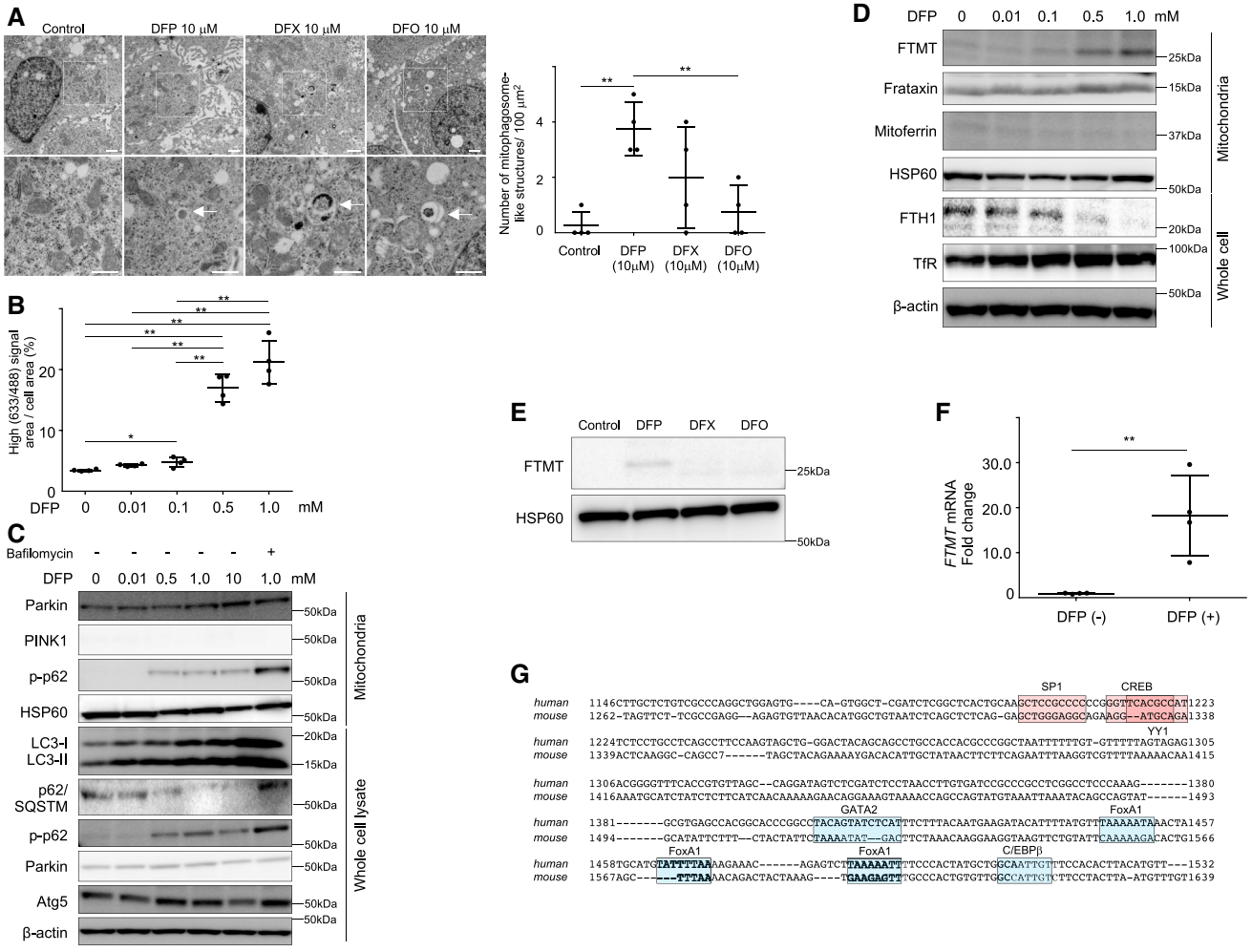

Figure EV1. Induction of mitophagy and FTMT by deferiprone, and a putative promoter region in *FTMT*.

A Electron microscopic images of Huh7 cells that were untreated or treated with DFP, DFX, or DFO. Boxed areas (×2,000) are enlarged below (×6,000). The white arrows indicate mitophagosome-like structures. Scale bar: 2.0 nm. The number of mitophagosome-like structures/100 μm^2 was compared for four randomly selected areas (technical replicates) between groups. The central horizontal bar and the error bars indicate mean ± SD. Tukey's honestly significant test was used for statistical analysis. $^{**}P < 0.01$.

B Quantification of mitophagy using mt-mKeima transfection and FACS analysis for HepG2 cells treated with DFP (0, 0.01, 0.5, or 1.0 mM as indicated) (n = 4, biological replicates). The central horizontal bar and the error bars indicate mean ± SD. Tukey's honestly significant test was used for statistical analysis. $^{*}P < 0.05$, $^{**}P < 0.01$.

C Immunoblots for Parkin, PINK1, phosphorylated p-62 (p-p62), HSP60, LC3, p62/SQSTM, and Atg5 using the mitochondrial fraction and whole cell lysates of HepG2 cells. HSP60 and β-actin were used as loading controls for mitochondrial and whole cell lysates, respectively.

D Immunoblots for mitochondria ferritin (FTMT), frataxin, mitoferrin, ferritin heavy chain (FTH1), and transferrin receptor (TfR) using the mitochondrial fraction and whole cell lysates of HepG2 cells following treatment with DFP (0, 0.01, 0.1, 0.5, or 1.0 mM as indicated). HSP60 and β-actin were used as loading controls for mitochondrial and whole cell lysates, respectively.

E Immunoblots for FTMT using the mitochondrial fraction lysate of Huh7 cells treated without or with iron chelators (DFP, DFX, or DFO). HSP60 was used as loading control.

F The mRNA expression of *FTMT* was quantified by real-time RT-PCR before and after DFP (1.0 mM) treatment (n = 4, biological replicates) in HepG2 cells. The mRNA expression of *FTMT* was normalized to *GAPDH*. The central horizontal bar and the error bars indicate mean ± SD. Two-sample t-test was used for statistical analysis. $^{**}P < 0.01$.

G A representation of the reported transcription factors for the mitochondrial ferritin promoter (Guaraldo *et al*, 2016). The locations of putative binding sites for transcription are boxed: Positive transcription factors (SP1, CREB, and YY1) are in red, while negative transcription factors (GATA2, FoxA1, and C/EBPβ) are in blue.

Source data are available online for this figure.

© 2020 The Authors

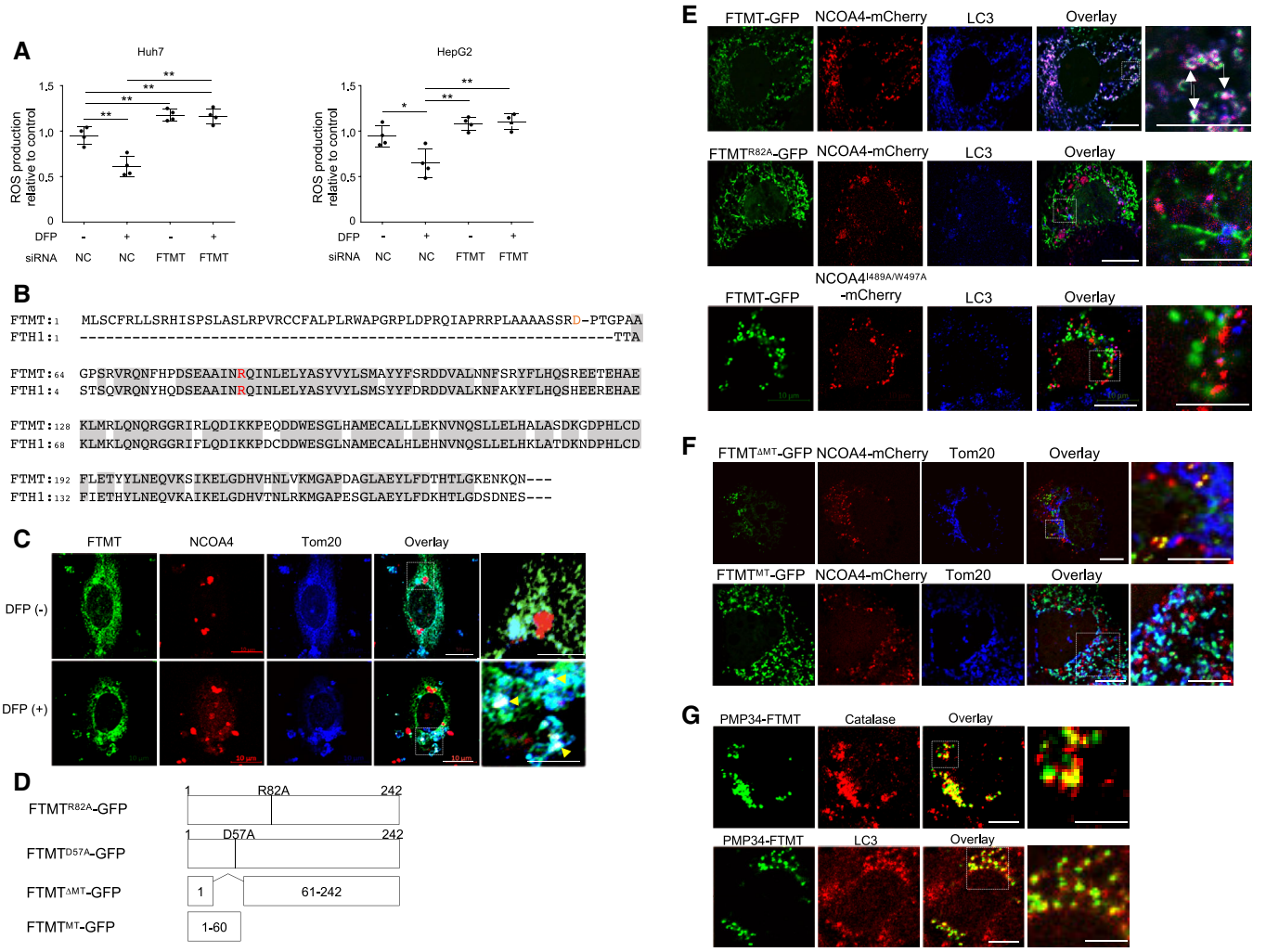

Figure EV2. Effects of FTMT knockdown on reactive oxygen species (ROS) production *in vitro*, the interaction of FTMT with NCOA4, and peroxisome-specific autophagy by FTMT with a peroxisome-targeting sequence.

A The cellular reactive oxygen species (ROS) levels were measured by oxidation of the cell-permeable and oxidation-sensitive fluorogenic precursor, 2,7-dihydrodichlorofluorescein diacetate for Huh7 cells (left), and HepG2 cells (right) with or without silencing of FTMT by siRNA (n = 4, biological replicates). DFP (−): without DFP, DFP (+): with 1 mM of DFP. The central horizontal bar and the error bars indicate mean ± SD. Tukey's honestly significant test was used for statistical analysis. *P < 0.05, **P < 0.01.

B Reported alignment of human FTMT and FTH1 amino acids (Levi *et al*, 2001). FTH1 R23 corresponds to R82 of FTMT. The orange "D" indicates the predicted cleavage site of the leader peptide of FTMT. The gray boxes represent the overlapping coding region where amino acid sequence of FTMT is identical to FTH1.

C Immunofluorescence staining for Tom20 (blue), NCOA4 (red), and endogenous FTMT (green) in normal human hepatocytes before and after DFP (1 mM) treatment. Boxed area is enlarged on the right. Scale bar: 10 and 5 μm in enlarged images. The white puncta by yellow arrowheads indicate the colocalization of FTMT, NCOA4, and Tom20.

D Schematic representation of GFP-tagged FTMT^{R82A}, FTMT^{D57A}, FTMT$^{\Delta MT}$, and FTMT^{MT}.

E Immunofluorescence staining for NCOA4-mCherry (red), NCOA4$^{I489A/W497A}$-mCherry (red), FTMT-GFP (green), FTMT^{R82A}-GFP (green), and LC3 (blue) in Huh7 cells. The white puncta shown by white arrows in the overlaid picture indicate the colocalization of FTMT-GFP, NCOA4-mCherry, and LC3. Boxed areas are enlarged on the right. Scale bar: 10 and 5 μm in enlarged images.

F Immunofluorescence staining for the mitochondrial target sequence-deleted FTMT-GFP (FTMT$^{\Delta MT}$-GFP) (green), FTMT mitochondrial target sequence-GFP (FTMT^{MT}-GFP) (green), NCOA4-mCherry (red), and Tom20 (blue) in Huh7 cells. Boxed areas are enlarged on the right. The yellow puncta and cyan puncta in the overlaid pictures indicate the colocalization of FTMT$^{\Delta MT}$-GFP and NCOA4-mCherry and the colocalization of FTMT^{MT}-GFP and Tom20, respectively. Scale bar: 10 μm and 5 μm in enlarged images.

G Immunofluorescence staining for catalase (red), PMP34-FTMT-GFP that has the peroxisome-targeting sequence instead of the mitochondria-targeting sequence (green), and LC3 (red) in Huh7 cells. The yellow puncta in the overlaid pictures indicate the colocalization of catalase and PMP34-FTMT-GFP or the colocalization of LC3 and PMP34-FTMT-GFP. Boxed areas are enlarged below. Scale bar: 10 and 5 μm in enlarged images.

© 2020 The Authors

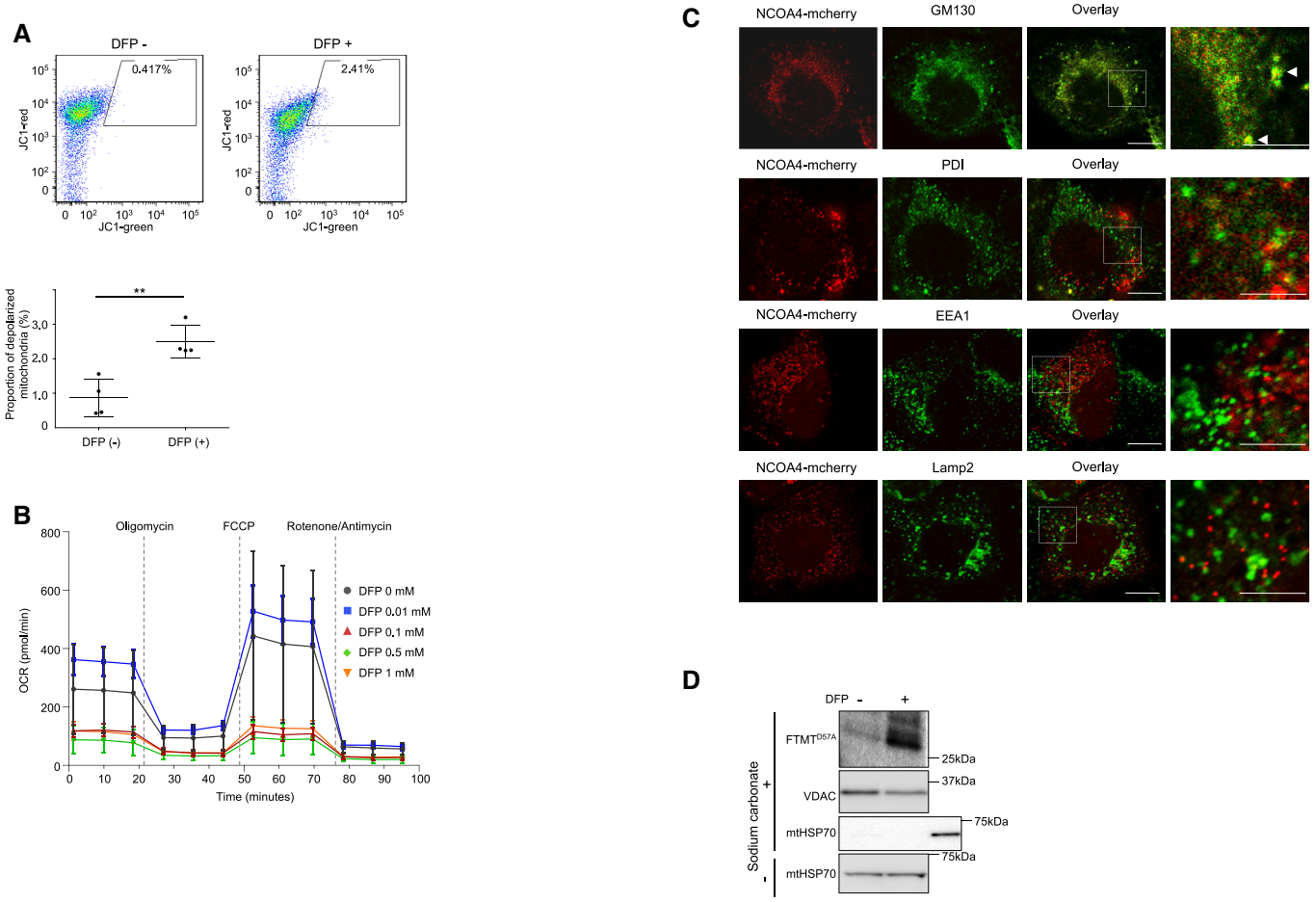

Figure EV3. Induction of mitochondrial damage by deferiprone, cytoplasmic localization of NCOA4, and FTMT^{D57A} precursor form in the mitochondrial membrane isolated from FTMT^{D57A}-expressing cells.

A Flow cytometric analysis of the mitochondrial membrane potential of the isolated mitochondria. The isolated mitochondria from HepG2 cells with or without DFP treatment were incubated with JC-1 for 1 h at 30°C and subjected to the flow cytometric analysis (n = 4, biological replicates) by excitation with a blue laser (488 nm) with emission assessed simultaneously using a 585/42 for JC-1 red and a 530/30 for JC-1 green. The trapezoid areas show the population of depolarized mitochondria. Quantification of the proportion of depolarized mitochondria is presented in the lower panel. The central horizontal bar and the error bars indicate mean ± SD. Two-sample t-test was used for statistical analysis. $^{**}P < 0.01$.

B The oxygen consumption rate was measured using a Seahorse XF24 Extracellular Flux Analyzer. Huh7 cells were incubated with different concentrations of DFP (0, 0.01, 0.1, 0.5, and 1 mM) for 24 h (n = 4, technical replicates). Oxygen consumption was measured, and the respiration rate was analyzed by injecting of 1 μM oligomycin, 1 μM carbonyl cyanide 4-(trifluoromethoxy)phenylhydrazone (FCCP), and 10 μM rotenone/antimycin A. The central point and the error bars indicate mean ± SD. OCR: oxygen consumption rate.

C Immunofluorescence staining for NCOA4-mCherry, GM130, protein disulfide isomerase (PDI), early endosome antigen 1 (EEA1), and Lamp2 in Huh7 cells. White arrowheads in the overlaid picture indicate the colocalization of NCOA4-mCherry and GM130. Boxed areas are enlarged on the right. Scale bar: 10 and 5 μm in enlarged images.

D Immunoblots for FTMT^{D57A} and VDAC using the mitochondrial membrane from Huh7 cells expressing FTMT^{D57A} with or without DFP treatment. The mitochondrial membrane was fractionated from cells by sodium carbonate treatment. mtHSP70 was used as the non-membrane-integral protein control and VDAC as the membrane-integral protein control. mtHSP70 at the right-hand side in the third lane indicates the positive control obtained from the mitochondrial fraction of Huh7 cells without DFP treatment.

Source data are available online for this figure.

© 2020 The Authors

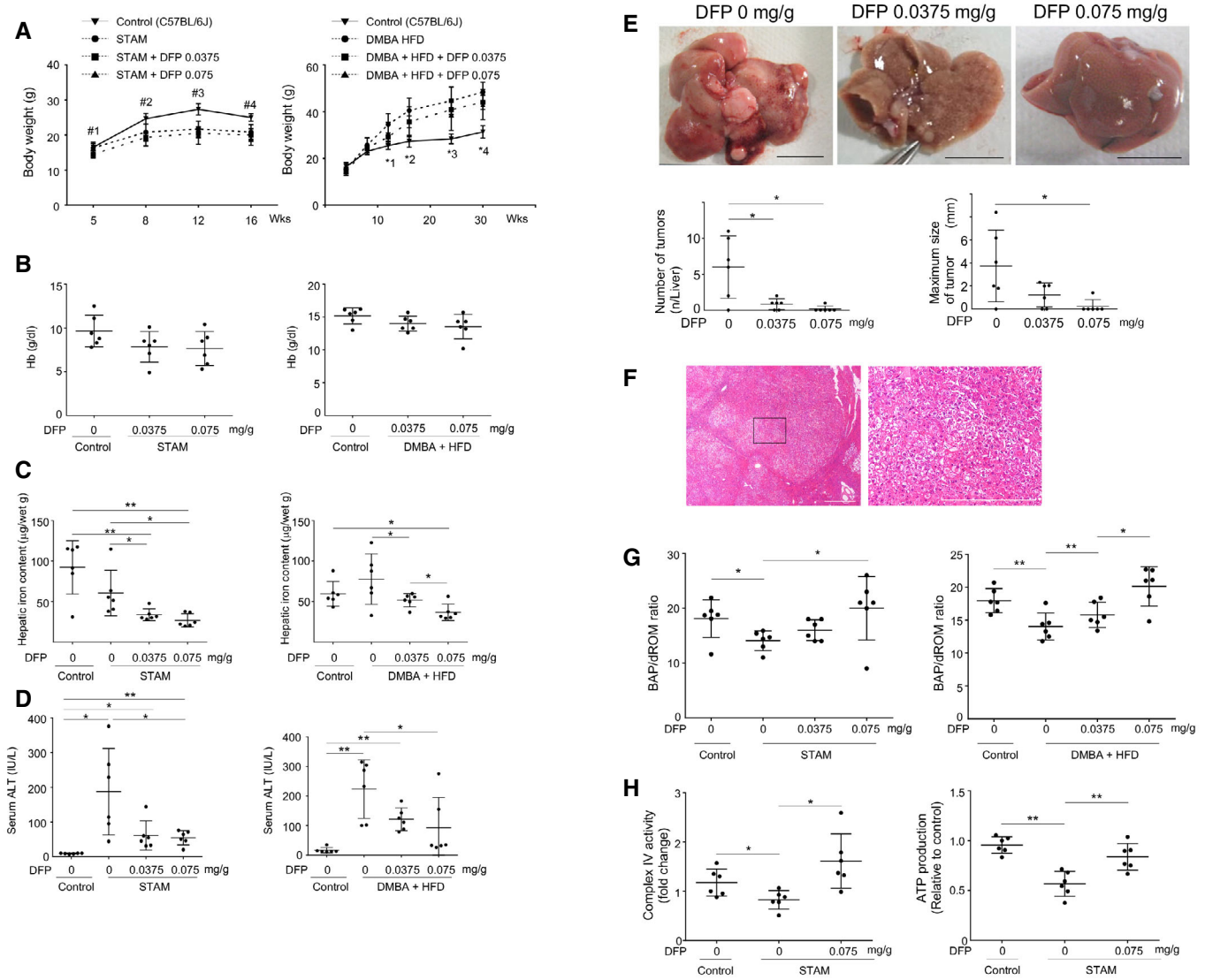

Figure EV4.

© 2020 The Authors

Figure EV4. Effects of DFP on body weight, hemoglobin level, hepatic iron content, ATL level, oxidative stress, and tumor growth in mice.

A Changes in body weights of untreated control (C57BL/6J, $n = 6$) mice, STAM mice ($n = 6$ for each group), and DMBA + HFD mice ($n = 6$ for each group) that were untreated or orally administered DFP as indicated (0, 0.0375, or 0.075 mg/g body weight) for 12 weeks (STAM mice) and for 26 weeks (DMBA + HFD mice). The central point and the error bars indicate mean ± SD. Tukey's honestly significant test was used for statistical analysis. #1: $P < 0.05$, control vs. STAM + DFP (0.0375 or 0.075), #2: $P < 0.01$, control vs. other 3 groups, #3: $P < 0.01$, control vs. other 3 groups, #4: $P < 0.01$, control vs. other 3 groups, *1: $P < 0.05$, control vs. DMBA HFD + DFP (0.0375), *2: $P < 0.05$, control vs. other 3 groups, *3: $P < 0.01$, control vs. other 3 groups, *4: $P < 0.01$, control vs. other 3 groups.

B Hemoglobin levels in untreated control (C57BL/6J) ($n = 6$) mice, STAM mice ($n = 6$ for each group), and DMBA + HFD mice ($n = 6$ for each group) that were orally administered DFP as described in (A). The central horizontal bar and the error bars indicate mean ± SD.

C Hepatic iron content in untreated control (C57BL/6J) mice ($n = 6$), STAM mice ($n = 6$ for each group), and DMBA + HFD mice ($n = 6$ for each group) that were untreated or orally administered DFP as described in (A). Hepatic iron content was determined by atomic absorption spectrometry and expressed as micrograms Fe per gram of tissue (wet weight). The central horizontal bar and the error bars indicate mean ± SD. Tukey's honestly significant test was used for statistical analysis. *$P < 0.05$, **$P < 0.01$.

D Serum ALT levels in untreated control (C57BL/6J) mice ($n = 6$), STAM mice ($n = 6$ for each group), and DMBA + HFD mice ($n = 6$ for each group) that were untreated or administered DFP as described in (A). The central horizontal bar and the error bars indicate mean ± SD. Tukey's honestly significant test was used for statistical analysis. *$P < 0.05$, **$P < 0.01$.

E The number and maximum size of liver tumors in DMBA + HFD mice ($n = 6$ for each group) that were untreated or orally administered DFP as described in (A). The central horizontal bar and the error bars indicate mean ± SD. Tukey's honestly significant test was used for statistical analysis. Representative images are shown in the upper panel. Scale bar: 1.0 cm. *$P < 0.05$.

F H&E staining of hepatocellular carcinoma in DMBA + HDF mice without DFP treatment. The tumor shows an increased cell density, an increased ratio of the nucleus to the cytoplasm, and thickened trabeculae (H&E stain). Scale bar: 100 μm.

G The ratio of biological antioxidant potential (BAP) to diacron reactive oxygen metabolites (dROM), which indicates systemic antioxidant potential, was measured in untreated control (C57BL/6J) mice ($n = 6$), STAM mice ($n = 6$ for each group), and DMBA + HFD mice ($n = 6$ for each group) that were untreated or orally administered DFP as described in (A). The central horizontal bar and the error bars indicate mean ± SD. Tukey's honestly significant test was used for statistical analysis. *$P < 0.05$, **$P < 0.01$.

H Mitochondrial complex IV activity and ATP production in untreated control (C57BL/6J) mice ($n = 6$) and STAM mice ($n = 6$ for each group) that were untreated or administered with 0.75 mg/g body weight of DFP for 12 weeks. Mitochondrial complex IV activity (left panel) was measured using the hepatic mitochondrial fraction. ATP production (right panel) was measured in liver homogenates. The central horizontal bar and the error bars indicate mean ± SD. Tukey's honestly significant test was used for statistical analysis. *$P < 0.05$, **$P < 0.01$.

© 2020 The Authors

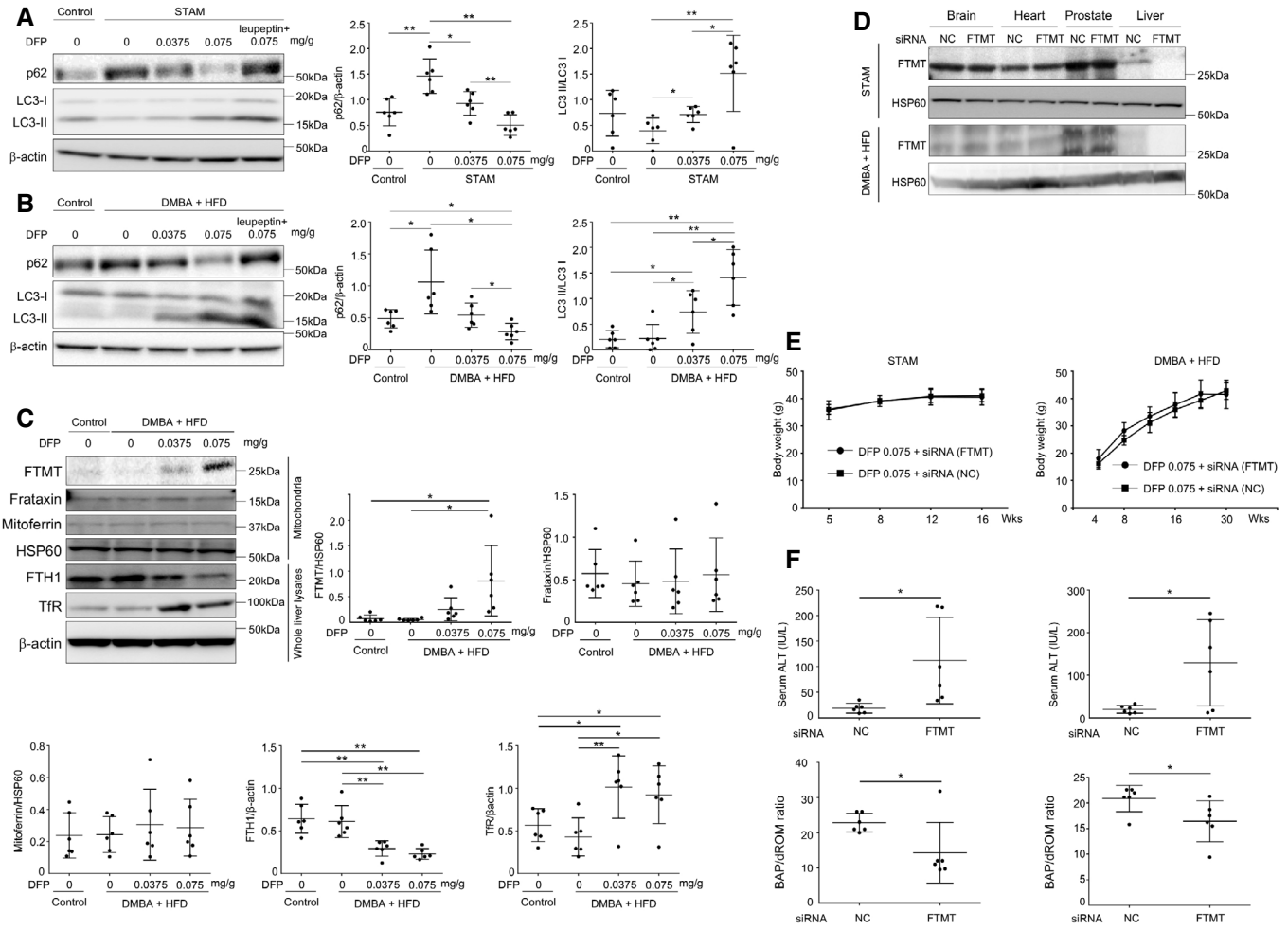

Figure EV5. Effects of DFP on autophagic flux and FTMT induction, and effects of FTMT knockdown on body weight, ATL level, and oxidative stress in mice.

A Immunoblots for p62 and LC3 using whole liver lysates from untreated control (C57BL/6J) mice and STAM mice treated with DFP (0, 0.0375, or 0.075 mg/g body weight) or DFP (0.075) + leupeptin (n = 6 for each group, biological replicates). The expression levels of p62 were normalized to β-actin, and LC3-II was normalized to LC3-I. The central horizontal bar and the error bars indicate mean ± SD. Tukey's honestly significant test was used for statistical analysis. *$P < 0.05$, **$P < 0.01$.

B Immunoblots for p62 and LC3 using whole liver lysates from untreated control (C57BL/6J) mice and DMBA + HFD mice treated with DFP (0, 0.0375, or 0.075 mg/g body weight) or DFP (0.075) + leupeptin (n = 6 for each group, biological replicates). The expression levels of p62 were normalized to β-actin, and LC3-II was normalized to LC3-I. The central horizontal bar and the error bars indicate mean ± SD. Tukey's honestly significant test was used for statistical analysis. *$P < 0.05$, **$P < 0.01$.

C Immunoblots for FTMT, frataxin, mitoferrin, HSP60, FTH1, and TfR using the hepatic mitochondrial fractions and whole liver lysates in control (C57BL/6J) mice and DMBA + HFD mice treated with DFP (0, 0.0375, or 0.075 mg/g body weight) (n = 6 for each group, biological replicates). The expression levels of FTMT, frataxin, and mitoferrin were normalized to HSP60, and those of FTH1 and TfR were normalized to β-actin. The central horizontal bar and the error bars indicate mean ± SD. Tukey's honestly significant test was used for statistical analysis. *$P < 0.05$, **$P < 0.01$.

D Immunoblots for FTMT using the mitochondrial fractions of brain, heart, prostate, and liver obtained from STAM mice and DMBA + HFD mice. Mice were orally administered 0.075 mg/g body weight of DFP for 12 weeks (STAM mice) or 26 weeks (DMBA + HFD mice) with administration of control siRNA or *FTMT* siRNA.

E Changes in body weights of STAM mice (n = 6) and DMBA + HFD mice (n = 6); both mouse models were treated as indicated in (D). The central point and the error bars indicate mean ± SD.

F ALT levels and the ratio of BAP to dROM in serum were measured in STAM mice (n = 6 for each group) (left panels) and DMBA + HFD mice (n = 6 for each group) (right panels). Both mouse models were treated as indicated in (D). The central horizontal bar and the error bars indicate mean ± SD. Two-sample t-test was used for statistical analysis. *$P < 0.05$.

Source data are available online for this figure.

© 2020 The Authors